small NANO MICRO

Molecular Junctions

Universal Scaling of the Charge Transport in Large-Area Molecular Junctions

*Auke J. Kronemeijer, Ilias Katsouras, Eek H. Huisman, Paul A. van Hal, Tom C. T. Geuns, Paul W. M. Blom, and Dago M. de Leeuw**

Charge transport through alkanes and para-phenylene oligomers is investigated in large-area molecular junctions. The molecules are self-assembled in a monolayer and contacted with a top electrode consisting of poly(3,4-ethylenedioxythiophene)–poly(4-styrenesulfonic acid) (PEDOT:PSS). The complete set of J(V,T) characteristics of both saturated and π-conjugated molecules can be described quantitatively by a single equation with only two fit parameters. The derived parameters, in combination with a variation of the bulk conductivity of PEDOT:PSS, demonstrate that the absolute junction resistance is factorized with that of PEDOT:PSS.

1. Introduction

Understanding of the charge transport in molecular devices is essential for progress in the field of molecular electronics. The two main fundamental challenges to resolve are the dependence of conductance on molecular length and the origin of the absolute value of the conductance.

A. J. Kronemeijer, I. Katsouras, E. H. Huisman, Prof. P. W. M. Blom, Prof. D. M. de Leeuw
Zernike Institute for Advanced Materials
University of Groningen
Nijenborgh 4, 9747 AG, Groningen, The Netherlands
E-mail: Dago.de.Leeuw@Philips.com

A. J. Kronemeijer
Optoelectronics Group
Cavendish Laboratory
University of Cambridge
J. J. Thomson Avenue, Cambridge CB3 0HE, UK

P. A. van Hal, T. C. T. Geuns, Prof. D. M. de Leeuw
Philips Research Laboratories
High Tech Campus 4, 5656 AE, Eindhoven, The Netherlands

Prof. P. W. M. Blom
TNO Holst Centre
High Tech Campus 31
5605 KN, Eindhoven, The Netherlands

Dr. E. H. Huisman
Center for Electron Transport in Molecular Nanostructures
Columbia University
500 W 120th St., New York, NY 10027, USA

DOI: 10.1002/smll.201100155

Charge transport through single molecules has been determined in break junctions and in scanning probe geometries. For short alkanes and π-conjugated molecules an increase in the molecular length L results in an exponential increase in resistance, $R \propto \exp(\beta L)$. The tunneling decay coefficient β depends on the energy gap between the highest occupied molecular orbital (HOMO) and the lowest unoccupied molecular orbital (LUMO).[1,2] The resistance is temperature-independent, which points to tunneling as the dominant transport mechanism.[3] For longer π-conjugated molecules (>3 nm), a transition to temperature-dependent hopping conduction has been reported.[4]

The absolute value of the resistance is ideally only determined by the molecular structure. However, in reality, the electrical contacts to the molecule strongly influence the measured resistance.[1,2,5–7] Firstly, strongly coupled chemisorbed contacts yield lower resistances than weakly coupled physisorbed contacts.[2,8,9] Secondly, the metal work function and the composition of the chemical anchoring group change the resistance.[9–12] Finally, differences in the coordination geometry of the chemical anchoring group at the metallic contact affect the resistance by virtue of a different electronic coupling.[13,14] Scanning probe geometries and break junctions[2,15] exhibit different coupling strengths to the contacts and therefore lead to dissimilar resistances for identical molecules. Hence an understanding of the electrical contacts is necessary to compare molecular conductance measurements.

To apply and integrate molecules into functional devices, macroscopic electrodes, preferably in a cross-bar geometry, are required. For this purpose we have developed large-area

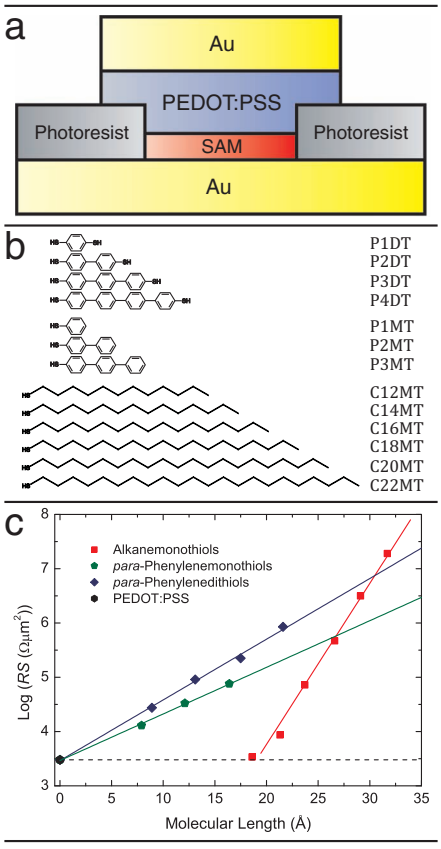

Figure 1. a) Schematic representation of the geometry of a large-area molecular junction. b) Chemical structures of the molecules investigated and their abbreviations. c) Normalized resistance (*RS*) as a function of molecular length of the large-area molecular junctions. The dotted line represents the normalized resistance of the corresponding PEDOT:PSS-only diode.

molecular junctions using self-assembled monolayers (SAMs).[16,17] As a top electrode the conducting polymer poly(3,4-ethylenedioxythiophene)–poly(4-styrenesulfonic acid) (PEDOT:PSS) is used. The geometry of the junction is schematically depicted in **Figure 1**a. A SAM is formed on a gold bottom electrode inside a vertical interconnect defined in photoresist. Subsequently, PEDOT:PSS is spin-coated on top to make the electrical contact to the SAM. We have investigated saturated alkanes and conjugated *para*-phenylene oligomers with thiol or methyl end groups.[16–18] The current density–voltage (*J*–*V*) characteristics show clear molecular features as concluded from the exponential dependence of the junction resistance on molecular length. Tunneling decay coefficients for SAMs with thiol and methyl end groups have been determined as 0.26 and 0.20 $Å^{-1}$ for conjugated *para*-phenylenes and as 0.66 and 0.73 $Å^{-1}$ for saturated alkanes.[16–18]

The origin of the absolute value of the resistance nevertheless remains unclear. The resistance of the junction is influenced by the composition of the PEDOT:PSS formulation and by the type of photoresist used. The molecular length dependence, however, remains unaffected. The charge transport, therefore, has been described with a multibarrier tunneling model yielding a factorized resistance [Equation (1)]:

$$R = \frac{h}{2e^2}\,T^{-1} = 12.9k\Omega \cdot T_{\mathrm{Au-S}}^{-1} \cdot T_{\mathrm{Molecule}}^{-1} \cdot T_{\mathrm{SAM-PEDOT}}^{-1} \quad (1)$$

where T is the overall transmission probability and T_{Molecule}, $T_{\mathrm{Au-S}}$, and $T_{\mathrm{SAM-PEDOT}}$ are the transmission probabilities of the molecule, the Au–S bond, and the SAM/PEDOT contact, respectively.[17] The molecular transmission is exponentially dependent on molecular length, $T_{\mathrm{Molecule}} \propto \exp(-\beta L)$. However, a detailed understanding of the physics of $T_{\mathrm{Au-S}}$ and, especially, of $T_{\mathrm{SAM-PEDOT}}$ is missing. The SAM/PEDOT contact is difficult to study experimentally since the interface is buried inside the junction.

To analyze the electrical transport we first focused on large-area junctions without molecules, or so-called PEDOT:PSS-only diodes, as a reference.[19] The electrical transport was shown to exhibit a power-law dependence on *both* temperature and voltage, viz. $J \propto T^{\alpha}$ at low voltage ($eV << kT$) and $J \propto V^{\beta}$ at low temperature ($eV >> kT$), with $\beta = \alpha + 1$. Furthermore, all *J*–*V* curves at different temperatures can be normalized onto a single universal curve by plotting $J/T^{1+\alpha}$ versus eV/kT.[19] The universal curve is described by [Equation (2)]:

$$J = J_0\,T^{1+\alpha}\,\sinh\left(\Upsilon\frac{eV}{kT}\right)\left|\Gamma\left(1+\frac{\alpha}{2}+i\Upsilon\frac{eV}{\pi kT}\right)\right| \quad (2)$$

The parameter α is derived from the measurements, J_0 and γ are fit parameters, e is the elementary charge, k is the Boltzmann constant, and Γ is the Gamma function. Equation (2) has been derived for dissipative tunneling in a biased double-quantum well.[20,21] The electron tunnels between the two wells while coupled to an external heat bath of harmonic oscillators. The coupling can be due to, for instance, Coulomb interactions or polaronic effects. The origin of the scaling in the PEDOT:PSS-only diodes, however, remains elusive.

Herein, we analyze in the same way the current–voltage characteristics of molecular junctions based on saturated alkanes and π-conjugated *para*-phenylene oligomers. The chemical structure and acronyms are presented in Figure 1b. The combined voltage and temperature dependences have been measured. All junctions exhibit universal scaling of the $J(V,T)$ characteristics as described by Equation (2). The values of the derived parameters α, J_0, and γ are compared with those of the PEDOT:PSS-only diodes. The comparison shows that the resistance of the molecular junctions is factorized with the resistance of PEDOT:PSS. The additional factorization has been verified by deliberately varying the PEDOT:PSS conductance. Previously unresolved and poorly understood issues regarding large-area molecular junctions will be evaluated and discussed.

2. Results and Discussion

Large-area molecular junctions were fabricated with monothiol and dithiol *para*-phenylene oligomers (P1MT–P3MT, P1DT–P4DT) and with alkanemonothiols (C18MT, C20MT, C22MT), presented in Figure 1b, according to previously

NANO MICRO small

reported procedures.[16–18] Figure 1c shows the normalized resistance for the investigated alkanes and *para*-phenylene oligomers (Figure 1b) on a semilogarithmic scale as a function of the molecular length. For each series of molecules the resistance increases exponentially with molecular length. The tunneling decay coefficients β are similar to previously reported values.[16–18] Figure 1c shows that the resistance of the *para*-phenylene oligomers extrapolates to the PEDOT:PSS-only resistance. The alkane-based junctions do not extrapolate to zero molecular length. Below molecular lengths of ≈20 Å the resistance of the molecular junctions is indistinguishable from the PEDOT:PSS-only resistance. The offset might be explained by a series resistance in the order of the PEDOT:PSS-only resistance, as indicated by the dashed line in Figure 1c. The origin of the series resistance and the absence of the effect for the π-conjugated compounds are not yet understood. Preferential adsorption of the insulating aliphatic backbone of PSS on top of the alkanemonothiol monolayers by virtue of increased van der Waals interactions might explain the observation.

To understand the origin of the absolute value of the resistance, we performed a combined temperature- and voltage-dependent analysis of the measured electrical transport. **Figure 2**a shows, as a representative example, the temperature-dependent *J*–*V* measurements of a benzenedithiol (P1DT) junction from 300 K down to 25 K. The current density is symmetric versus bias voltage and nonlinear; the resistance decreases with increasing bias. Furthermore, the current density decreases when lowering the temperature. The current density at 0.1, 0.3, and 0.5 V bias is presented as a function of temperature in Figure 2b on a double logarithmic scale. The straight lines obtained indicate a clear power-law dependence on temperature. The slope decreases with increasing bias voltage.

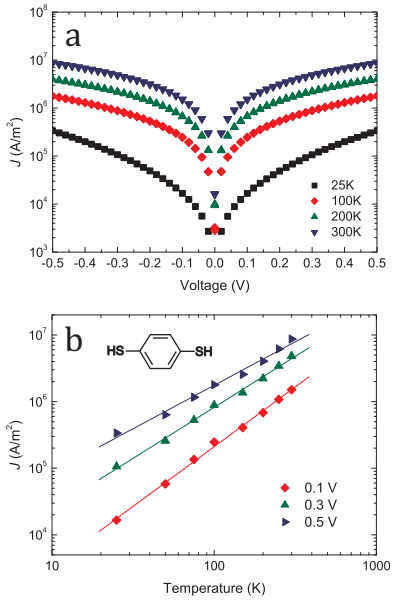

Figure 2. a) Current density as a function of bias for a benzenedithiol (P1DT)-based junction as measured at temperatures between 25 and 300 K. b) Current density of the P1DT junction at 0.1, 0.3, and 0.5 V bias as a function of temperature on a double logarithmic scale.

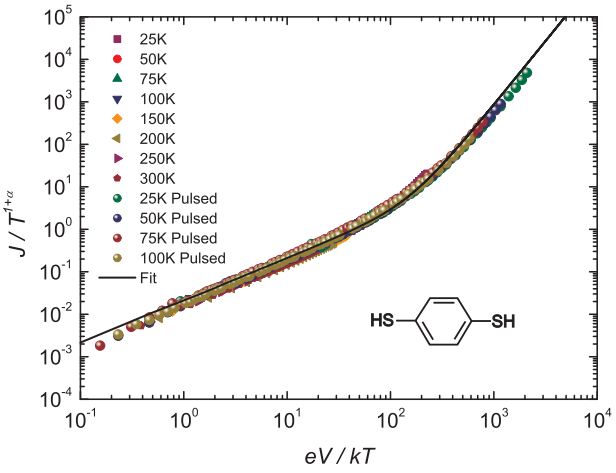

Figure 3. Scaled current density of a benzenedithiol (P1DT) junction presented on a double logarithmic scale as a function of eV/kT. Both dc measurements up to 0.5 V bias and pulse measurements up to 5 V are included. The solid curve is calculated with Equation (2) using $\alpha = 2.0$, $\gamma = 2.0 \times 10^{-2}$, and $J_0 = 1.1$ A m^{-2}.

Extrapolation of the value of the slope to 0 V bias where $kT >> eV$ yields the value of the parameter α. A value for α of 2.0 is obtained. The experimental data of Figure 2a can now be replotted as $J/T1^{+}\alpha$ versus eV/kT. **Figure 3** shows that a single, smooth curve is obtained, with eV/kT spanning four orders of magnitude and the scaled current density spanning seven orders of magnitude. The solid line is calculated with Equation (2); a good agreement is obtained. There are only two fit parameters J_0 and γ. The value of $\gamma = 2.0 \times 10^{-2}$ determines the position of the "knee" in the curve while $J_0 = 1.1$ A m^{-2} fixes the absolute value. The other π-conjugated molecules show a similar scaling of the normalized current density versus eV/kT.

Similar scaling was observed for the alkanemonothiol junctions as well. As a typical example, **Figure 4** shows the scaled current density as function of eV/kT for docosanemonothiol

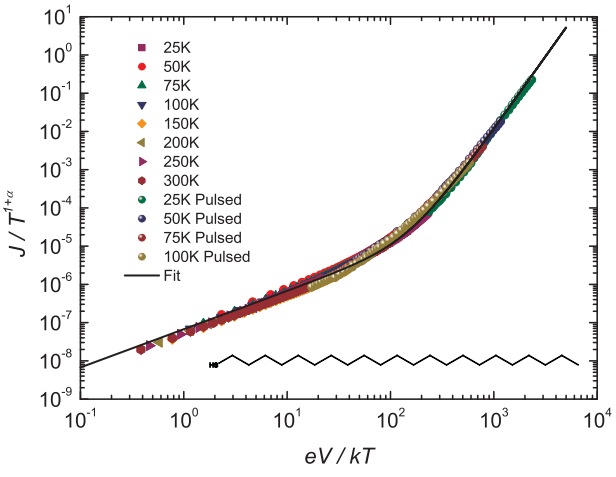

Figure 4. Scaled current density of a docosane (C22MT) junction presented on a double logarithmic scale as a function of eV/kT. Both dc measurements up to 0.5 V bias and pulse measurements up to 5 V are included. The solid curve is calculated with Equation (2) using $\alpha = 2.8$, $\gamma = 2.3 \times 10^{-2}$, and $J_0 = 1.9 \times 10^{-6}$ A m^{-2}.

Table 1. Parameters derived from the analysis of the electrical transport in large-area junctions by using Equation (2). The normalized resistance (*RS*), the power-law coefficient α, and the fit parameters J_0 and γ are shown. Furthermore, the value of $\pi\gamma^{-1}$, related to the number of microscopic tunneling events, is presented.

Junction type	$RS_{0.1V}$ [Ω μm²]	α	γ	$\pi\gamma^{-1}$	J_0 [A m^{-2}]
PEDOT:PSS	3.0×10^{3}	1.3	2.5×10^{-2}	126	2.0×10^{2}
P1DT	2.8×10^{4}	2.0	2.0×10^{-2}	157	1.1
P2DT	9.1×10^{4}	2.1	1.9×10^{-2}	165	1.3×10^{-1}
P3DT	2.2×10^{5}	2.3	2.3×10^{-2}	137	7.7×10^{-3}
P4DT	8.5×10^{5}	2.4	3.3×10^{-2}	95	1.3×10^{-3}
P1MT	1.3×10^{4}	2.4	2.4×10^{-2}	131	7.0×10^{-2}
P2MT	3.3×10^{4}	2.2	2.2×10^{-2}	143	2.2×10^{-1}
P3MT	7.6×10^{4}	1.9	2.1×10^{-2}	150	5.8×10^{-1}
C18MT	2.7×10^{5}	1.6	2.5×10^{-2}	126	1.8×10^{-1}
C20MT	8.4×10^{6}	3.0	2.2×10^{-2}	143	4.0×10^{-6}
C22MT	1.9×10^{7}	2.8	2.3×10^{-2}	137	1.9×10^{-6}

(C22MT). A single, smooth curve is found. The solid line is calculated by Equation (2) with $\alpha = 2.8$ and using fit constants γ of 2.3×10^{-2} and J_0 of 1.9×10^{-6} A m^{-2}. A good agreement is obtained. The observation of temperature dependence is in contrast with previous reports in which, from measurements down to 200 K, temperature-independent transport was claimed.[16] We note that a decisive statement can only be made when measurements to lower temperatures are performed. For the specific type of PEDOT:PSS used the power-law dependence resulted in only minor changes in the electrical characteristics down to 200 K. For lower temperatures, however, the temperature dependence progressively increases.

The complete $J(V,T)$ characteristics of all large-area molecular junctions can be described using only three parameters, viz. α, γ, and J_0. **Table 1** summarizes the values for all molecular junctions and for the corresponding PEDOT:PSS-only diode. Table 1 shows that the values of γ for the molecular junctions are nearly constant. Furthermore, they are identical to that of the PEDOT:PSS-only diode from which we conclude that the value of γ in the molecular junctions is determined by PEDOT:PSS. The normalized resistance for the junctions varies over four orders of magnitude whereas α varies only between 2.0 and 3.0. The value of α determines the temperature dependence at low bias. Table 1 shows that the values of α and γ are essentially constant and the main difference between the junctions is the value of the prefactor J_0. When α is exactly the same for all junctions, the prefactor should scale linearly with RS at low bias. When compensated for the small differences in α, a one-to-one correspondence is indeed found. When variations in α can be disregarded, J_0 depends exponentially on the molecular length. Therefore J_0 contains the molecular contribution.

The similarity between the molecular junctions and the PEDOT:PSS-only diode implies that the temperature and voltage dependence originates from the PEDOT:PSS. The molecular contribution is only a length-dependent prefactor. Furthermore, the similarity suggests that the prefactor J_0

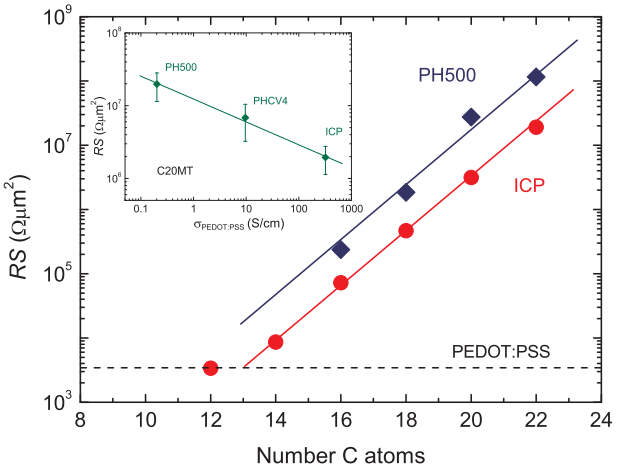

Figure 5. Normalized resistance versus molecular length of alkanemonothiol-based junctions fabricated with different PEDOT:PSS formulations. Data are reproduced from Reference [17]. The inset shows the normalized resistance of icosanemonothiol (C20MT) junctions versus the (four-point probe) conductivity of the PEDOT:PSS formulation used to fabricate the junctions.

scales with the PEDOT:PSS resistance. To verify this factorization we varied the conductivity of PEDOT:PSS between 0.2 and 300 S cm^{-1}. **Figure 5** presents the normalized resistance of alkanemonothiols as a function of molecular length for junctions containing two PEDOT:PSS formulations. For both series an identical length dependence is obtained. The difference is about an order of magnitude in the absolute value of the resistance. The inset of Figure 5 shows the dependence of the resistance of icosanemonothiol (C20MT) junctions on the bulk PEDOT:PSS conductivity. The obtained correlation implies that J_0 depends not only on the molecular length but also on the conductivity of PEDOT:PSS.

Consequently, in the multibarrier tunneling model for the large-area junctions the factorization with the PEDOT:PSS resistance has to be explicitly included [Equation (3)]:

$$R = 12.9k\Omega \cdot T_{\mathrm{Au-S}}^{-1} \cdot e^{\beta L} \cdot T_{\mathrm{SAM-PEDOT}}^{-1} \cdot T_{\mathrm{PEDOT:PSS}}^{-1} \qquad (3)$$

We note that a relation with the bulk conductivity of PEDOT:PSS has previously been suggested.[17] The current analysis unambiguously demonstrates this factorization.

Previously, we have used the Simmons model to interpret the electrical transport in molecular junctions.[22] A good description for the normalized resistance at low bias was obtained. At higher bias, however, the model underestimated the resistance. The discrepancy is due to the fact that the Simmons model is derived for an insulator sandwiched between two metallic electrodes. The current transport is by tunneling and depends exponentially on the applied bias. The transport in these large-area molecular junctions, however, is factorized with the PEDOT:PSS resistance. This polymer is a highly doped semiconductor and yields a power-law dependence on both bias and temperature.

NANO MICRO small

Factorization of the resistance of molecular junctions with PEDOT:PSS accounts for a number of previously poorly understood processing issues. The resistance of the junctions was shown to depend on the type of PEDOT:PSS used as contact and on the type of photoresist used to define the *vias*.[17] It has now been demonstrated that the influence stemming from PEDOT:PSS is actually the conductivity of the film. The dependence on the type of photoresist might be explained by differences in surface tension, which lead to a modified morphology of the PEDOT:PSS film, effectively modifying $T_{SAM-PEDOT}$.

For large-area junctions the current density is constant, that is, the current scales with device area. For *vias* with a diameter smaller than 5 μm deviations can occur. The wetting of PEDOT:PSS on the SAM is different from that on the photoresist. The electrical contact at the perimeter of the *vias* can be different from that in the middle. This nonhomogeneity increases with decreasing diameter of the *via*. Hence the larger the via, the better is the scaling.

The yield of junctions is in first order "digital", either 100 or 0%. A junction is called shorted when the resistance coincides with the PEDOT:PSS-only resistance. The resistance of the junction is given by Equation (3). The inverse transmission prefactors cannot be smaller than unity. Hence, the resistance cannot be smaller than that of a PEDOT:PSS-only diode. Any higher value is counted as a functional junction. The quality of a wafer is therefore not assessed by the yield but by the parameter spread.

The establishment of factorization and the dominant role of PEDOT:PSS on the transport in molecular junctions demonstrates that PEDOT:PSS cannot be regarded as a simple metallic electrode. Any change in the processing can yield different transmission factors and, hence, differences in the absolute value of the resistance. However, if the fabrication technology is strictly kept constant a clear signature of the molecular structure is observed. Consequently, large-area molecular junctions can yield valuable information on transport through functional molecules.

3. Conclusion

Charge transport through monolayers of alkanes and *para*-phenylene oligomers has been investigated in large-area molecular junctions. The molecules are self-assembled in a monolayer on a gold bottom electrode and contacted with a PEDOT:PSS top electrode. The current density exhibits a power-law dependence on both temperature and bias, viz. $J \propto T^{\alpha}$ at low voltage ($eV << kT$) and $J \propto V^{\beta}$ at low temperature ($eV >> kT$), with $\beta = \alpha + 1$. The value of α is unambiguously determined from the temperature dependence at low bias. For all molecules investigated replotting the scaled current density $J/T^{1+\alpha}$ as a function of eV/kT yields a single smooth curve spanning over orders of magnitude. With only two fit parameters, γ and J_0, the complete $J(V,T)$ characteristics can be quantitatively described. The prefactor J_0 depends on the molecular length. The values of α and γ are essentially constant for the molecular junctions and, furthermore, identical to those of the corresponding PEDOT:PSS-only diode. This similarity implies that the temperature and voltage dependence originates from PEDOT:PSS. The molecular contribution is only a length-dependent prefactor. Furthermore, by varying the type of PEDOT:PSS we have shown that J_0 depends on the bulk conductivity of PEDOT:PSS as well. Consequently, in a multibarrier tunneling model the factorization with the PEDOT:PSS resistance has to be explicitly included. The dominant role of the PEDOT:PSS contact explains the absolute value of the junction resistance and its relation to processing conditions.

4. Experimental Section

On a 6-inch Si monitor wafer with a 500-nm SiO_2 passivation layer, a 60-nm Au bottom electrode was sputtered onto a Ti adhesion layer and structured by standard photolithography. Vertical interconnects ranging from 1 to 100 μm in diameter were defined in photoresist. After development the photoresist was hard baked at 200 °C for at least 1 h to render it solvent-resistant. Residual contaminants on the bottom gold contacts were removed by an oxygen plasma. The gold became slightly oxidized and was afterwards reduced by soaking the wafer in ethanol.

SAMs were formed inside the vertical interconnects under a N_2 atmosphere. Alkanethiols were dissolved in ethanol at a concentration of 3×10^{-3} M and thiolated *para*-phenylene oligomers were dissolved in SureSeal THF at 3×10^{-4} M. The wafers were immersed in the solutions for 36 h. After self-assembly, the wafers were thoroughly rinsed with ethanol, toluene, and isopropanol to remove any remaining molecules.

Subsequently, the conducting polymer PEDOT:PSS, a water-based suspension of poly(3,4-ethylenedioxythiophene) stabilized with poly(4-styrenesulfonic acid), was spin-coated. PEDOT:PSS acts as a highly conductive layer that protected the SAM during evaporation of the top gold contact and prevents formation of shorts. After spin-coating, the layers were dried in a dynamic vacuum for at least 1 h. The layer thicknesses amounted to about 90 nm as measured with a Dektak surface profilometer. Three PEDOT:PSS formulations were used: Clevios PH500 (H. C. Starck), Clevios P HC V4 (H. C. Starck), and AGFA ICP new type (Agfa–Gevaert) mixed with 5% dimethyl sulfoxide (DMSO). The standard process flow chart was based on the AGFA ICP formulation. Next, auxiliary 100-nm gold top electrodes were thermally evaporated and structured by photolithography. To remove parasitic currents the redundant PEDOT:PSS was removed by reactive ion etching using an oxygen plasma. The top gold layer acted as a self-aligned etching mask.

The normalized resistance (*RS* in Ω μm^2) at 0.5 V bias was measured in four-point probe geometry in a semiautomatic probe station. Temperature-dependent *J–V* measurements down to 25 K were performed on a representative subset of molecular junctions. Measurements were performed in a cryogenic probe station (Janis Research Co.) equipped with a Keithley 4200 semiconductor parameter analyzer. Control measurements at room temperature were performed afterwards to exclude permanent damage to the diodes. At room temperature the bias window was limited to ≈1 V due to break down. At low temperatures (25–100 K), pulse measurements with a Keithley 2602 Source System controlled by a Labview program were used to increase the window up to 5 V. Pulse and dc measurements were identical in the overlapping bias voltage window.

Acknowledgements

The authors thank Jan Harkema for technical support and Sense Jan van der Molen for helpful discussions. We gratefully acknowledge financial support from NanoNed, a national nanotechnology program coordinated by the Dutch Ministry of Economic Affairs, from the Zernike Institute for Advanced Materials, and from the European Community Seventh Framework Programme FP7/2007-2013 project 212311, ONE-P.

[1] A. Salomon, D. Cahen, S. Lindsay, J. Tomfohr, V. B. Engelkes, C. D. Frisbie, *Adv. Mater.* **2003**, *15*, 1881.
[2] H. B. Akkerman, B. de Boer, *J. Phys. Condens. Matter* **2008**, *20*, 013001.
[3] W. Wang, T. Lee, M. A. Reed, *Phys. Rev. B* **2003**, *68*, 035416.
[4] S. H. Choi, B. Kim, C. D. Frisbie, *Science* **2008**, *320*, 1482.
[5] K. W. Hipps, *Science* **2001**, *294*, 536.
[6] J. G. Kushmerick, *Mater. Today* **2005**, *8*, 26.
[7] D. Vuillaume, S. Lenfant, *Microelectron. Eng.* **2003**, *70*, 539.
[8] X. D. Cui, A. Primak, X. Zarate, J. Tomfohr, O. F. Sankey, A. L. Moore, T. A. Moore, D. A. Gust, G. Harris, S. M. Lindsay, *Science* **2001**, *294*, 571.
[9] V. B. Engelkes, J. M. Beebe, C. D. Frisbie, *J. Am. Chem. Soc.* **2004**, *126*, 14287.
[10] F. Chen, X. Li, J. Hihath, Z. Huang, N. Tao, *J. Am. Chem. Soc.* **2006**, *128*, 15874.
[11] J. M. Beebe, V. B. Engelkes, L. L. Miller, C. D. Frisbie, *J. Am. Chem. Soc.* **2002**, *124*, 11268.
[12] Y. S. Park, A. C. Whalley, M. Kamenetska, M. L. Steigerwald, M. S. Hybertsen, C. Nuckolls, L. Venkataraman, *J. Am. Chem. Soc.* **2007**, *129*, 15768.
[13] X. Li, J. He, J. Hihath, B. Xu, S. M. Lindsay, N. Tao, *J. Am. Chem. Soc.* **2006**, *128*, 2135.
[14] C. Li, I. Pobelov, T. Wandlowski, A. Bagrets, A. Arnold, F. J. Evers, *J. Am. Chem. Soc.* **2008**, *130*, 318.
[15] B. A. Mantooth, P. S. Weiss, *Proc. IEEE* **2003**, *91*, 1785.
[16] H. B. Akkerman, P. W. M. Blom, D. M. de Leeuw, B. de Boer, *Nature* **2006**, *441*, 69.
[17] P. A. van Hal, E. C. P. Smits, T. C. T. Geuns, H. B. Akkerman, B. C. de Brito, S. Perissinotto, G. Lanzani, A. J. Kronemeijer, V. Geskin, J. Cornil, P. W. M. Blom, B. de Boer, D. M. de Leeuw, *Nat. Nanotechnol.* **2008**, *3*, 749.
[18] A. J. Kronemeijer, E. H. Huisman, H. B. Akkerman, S. M. Goossens, I. Katsouras, P. A. van Hal, T. C. T. Geuns, S. J. Van Der Molen, P. W. M. Blom, D. M. de Leeuw, *Appl. Phys. Lett.* **2010**, *97*, 173302.
[19] A. J. Kronemeijer, E. H. Huisman, I. Katsouras, P. A. van Hal, T. C. T. Geuns, P. W. M. Blom, S. J. Van Der Molen, D. M. de Leeuw, *Phys. Rev. Lett.* **2010**, *105*, 156604.
[20] H. Grabert, U. Weiss, *Phys. Rev. Lett.* **1985**, *54*, 1605.
[21] M. P. A. Fisher, A. T. Dorsey, *Phys. Rev. Lett.* **1985**, *54*, 1609.
[22] H. B. Akkerman, R. C. G. Naber, B. Jongbloed, P. A. van Hal, P. W. M. Blom, D. M. de Leeuw, B. de Boer, *Proc. Natl. Acad. Sci. USA* **2007**, *104*, 11161.

Received: January 24, 2011
Revised: March 7, 2011
Published online: April 28, 2011